COMPUTATIONAL STUDY ON THE CYCLIC LOADING BEHAVIOR OF STEEL CHEVRON BRACED FRAMES IN JAPAN

I. Dias[1], T. Okazaki[2], A. Seki[3]

[1] Graduate student, Graduate School of Engineering, Hokkaido University, Sapporo, 060-8628, Japan. Email: ilanildodias@gmail.com
[2] Professor, Faculty of Engineering, Hokkaido University, Sapporo, 060-8628, Japan. Email: tokazaki@eng.hokudai.ac.jp
[3] Graduate student, Graduate School of Engineering, Hokkaido University, Sapporo, 060-8628, Japan. Email: garagohho@eis.hokudai.ac.jp

Abstract

A typical steel braced frame in Japan places a pair of diagonal braces in a chevron (or inverted V) arrangement within a moment-resisting frame (MRF). Despite being widely used, limited design guidance is available in the Japanese code provisions and recommendations, and consequently, a wide range of different design choices are adopted in practice. In order to examine the seismic performance of such steel braced frames, a combined experimental and computational study was conducted. This paper reports the computational part of the study.

Nonlinear finite element method (FEM) models were validated against data and observations from six chevron braced-frame specimens. The validated FEM models were used to conduct a parametric study to further understand how the seismic behavior of chevron braced frames may be affected by the relative strength of the beam with respect to braces. The computation results suggest that in order to strictly prevent yielding of the beam intersecting braces, chevron braced-frames must be proportioned such that at least 60% of the lateral strength is derived from moment-frame action and no more than 40% from the braces. For cases where this limit is exceeded, the beam functions as source of energy dissipation mechanism as it undergoes severe inelastic deflection. The findings are examined over a practical range of brace angles and member proportions.

Nonlinear time history analysis of a 4-story building was conducted to examine the seismic performance of chevron CBFs in Japan. The range of different mechanisms assumed in the engineering practice, different connection types, and different possible β examined in this study all led to adequate performance. All models remained within story drift of 0.02 rad for ground motions whose elastic acceleration response spectrum was up to 1.2g at the fundamental vibration frequency. For β = 0.35, regardless of the mechanism assumed in design, the strong-beam mechanism controlled.

Keywords: steel structures; seismic performance; concentrically braced frames; design methods; finite element method.

1. Introduction

Steel concentrically braced frames (CBFs) are widely used in high seismicity regions due to their large elastic stiffness and strength. Engineers often choose to place braces in a "chevron" arrangement to meet architectural requirements. A typical Japanese steel CBF places chevron braces within a moment-resisting frame (MRF). In such CBFs, the beam must be designed for the unbalanced force between the braces combined with moment-frame action. Experiments by Shibata and Wakabayashi [1] and Yamanouchi et al. [2] demonstrated that if the beam yields before the tension brace, then beam yielding instead of brace yielding may dictate the seismic behavior of the CBF. Fukuta et al. [3] proposed a design rule to proportion such beam intersecting braces. Similarly, Khatib et al. [4] explained that depending on the relative strength of the beam with respect to the braces, chevron CBFs can fail in one of two mechanisms, the "strong-beam" mechanism or the "weak-beam" mechanism as depicted in Fig. 1. The weak-beam mechanism will form if the beam yields due to the force unbalance before the tension brace develops its yield strength. The strong-beam mechanism will form if the tension brace develops its yield strength while the beam remains elastic. Khatib et al. [4] and Tremblay and Roberts [5] stated that the weak-beam mechanism is undesirable for multi-story structures because severe strength degradation caused by such mechanism can lead to soft story formation. North American design provisions [6] require proportioning the beam intersecting braces to remain elastic under the condition that the tension brace develops its yield strength and compression brace carry a small portion of its original strength.

In Japan, limited design guidance has been offered by the Japanese codes and provisions on the proportioning and detailing of chevron CBFs. Engineers have employed a wide variety of different design rules. Therefore, a combined experimental and computational study was conducted to examine the seismic performance of chevron CBFs designed and constructed according to the current practice in Japan [8]. This paper summarizes the computational component of the project whose objective was to further the understanding obtained from the experimental observations and to examine the effect of primary design parameters on the performance of chevron CBFs, in particular, the proportion of lateral load carried by the braces and the relative strength of the beam with respect to the braces.

2. Design Equations

A key design parameter of chevron CBFs is the proportion of ultimate lateral strength derived from the braces with respect to that of the entire system, β. This factor dictates the ductility category of CBFs in the Japanese building code [8]. As depicted in Fig. 2, a chevron CBF may be decomposed into a pair of braces, placed in angle α, and a moment-resisting frame. In the following analysis, the column is assumed to remain elastic except at the bases. The plastic strength of the combined system, H, may be evaluated as the sum of the contribution of the MRF, H_f, and that derived from the braces, H_b, and thereby $\beta = H_b/H$. Depending on the relative strength of the braces with respect to the beam, the tension brace may develop its yield strength N_y, hereinafter referred as "strong-beam" mechanism (see Fig. 1a), or else the beam may yield under the action of reverse end moments and force unbalance between the braces, referred as "weak-beam" mechanism (see Fig. 1b). In the latter case, the force carried by the tension brace, N_t, is limited by the strength of the beam and will not reach N_y.

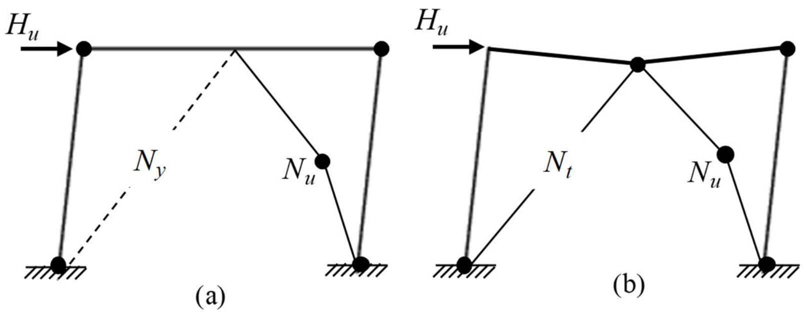

Fig. 1 – Collapse mechanism of chevron CBFs: a) Strong beam; b) Weak beam

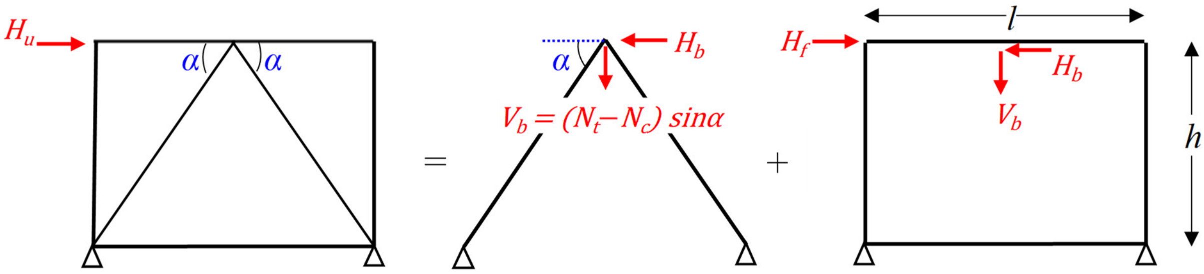

Fig. 2 – Structural model decomposed into pair of braces and moment-resisting frame

For the two cases, the factor β is expressed as follows:

For strong-beam mechanism: $\beta = ((1+x)\,r) / (1 + (1+x)\,r)$ (1)

For weak-beam mechanism: $\beta = ((\kappa/2) + 2xr) / (1.5 + 2xr)$ (2)

In the above equation, $r = (N_y\,h \cos\alpha)/(4M_p)$ is a measure of the relative horizontal strength of the braces with respect to the beam, $x = N_u / N_y$ is the compressive to tensile strength ratio of the brace, and κ, $1 \le \kappa \le 2$, is the limiting value for the ratio of the maximum possible force unbalance, $V_b = (N_y - N_u)\sin\alpha$, over the plastic resistance of the beam, $4M_p/l$, when subject to reverse end moments M_p. Furthermore, M_p is the plastic strength of the beam, and N_u is the reduced strength of the brace after cyclic loading. In this study, N_u is computed as one third of the compressive strength at buckling. A key issue is that κ is not constant during the inelastic loading process. The most favorable condition for controlling the weak-beam mechanism is κ = 2, which corresponds to the condition when the end moments M_p act in the same direction to oppose the force unbalance. Strong-beam mechanism controls when $r \le \kappa / (2(1 - x))$ and weak-beam mechanism controls otherwise.

The relationship between β and r shall provide a useful design guide for engineers. Fig. 3 shows an example computed for α = 57° (which is identical to the specimens discussed in the following chapter) and λ = 40, 80 and 120. Two cases, κ = 1 and 1.5 are considered. The figure indicates that, if inelastic deflection of the beam intersecting braces is to be strictly avoided (κ < 1), β is at most 0.4. If limited yielding of the beam is permitted ($1 \le \kappa \le 1.5$), β may be as large as 0.7. Where the strong-beam mechanism controls, β is nearly

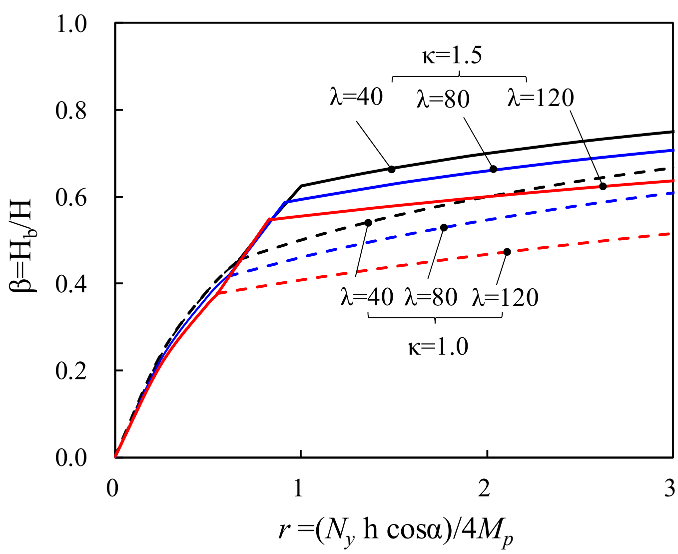

Fig. 3 – Proposed design equation for brace slenderness ratios λ=40, 80 and 120

proportional to *r*, in other words, larger braces lead to greater β. Where the weak-beam mechanism controls, stronger braces with smaller λ (and hence larger *x*) and larger *r* does not lead to proportionally larger β.

3. Experimental Program

Six large-scale CBF specimens were subjected to cyclic loading to understand the seismic performance of chevron CBFs [7]. As shown in Fig. 4, the specimen comprised a pair of braces placed in a single bay-single story MRF. The specimens represented 60% scale of a typical building structure. The specimens were identical in configuration and overall dimension but employed different brace sections and bracing connections. Three specimens used round-HSS braces while the other three used I-section braces. Four specimens adopted bolted bracing connections commonly used in Japan, and two specimens adopted a field-welded bracing connection designed following the balanced design procedure proposed by Roeder et al. [9]. Fig. 5 illustrates the bracing connections of Specimens 4 to 6 which will be discussed later. These three specimens used I-section braces. Specimen 5 oriented the brace to buckle in plane and the other two oriented the braces to buckle out of plane. Load was applied at the top of the north column according to a cyclic loading protocol up to a story-drift angle

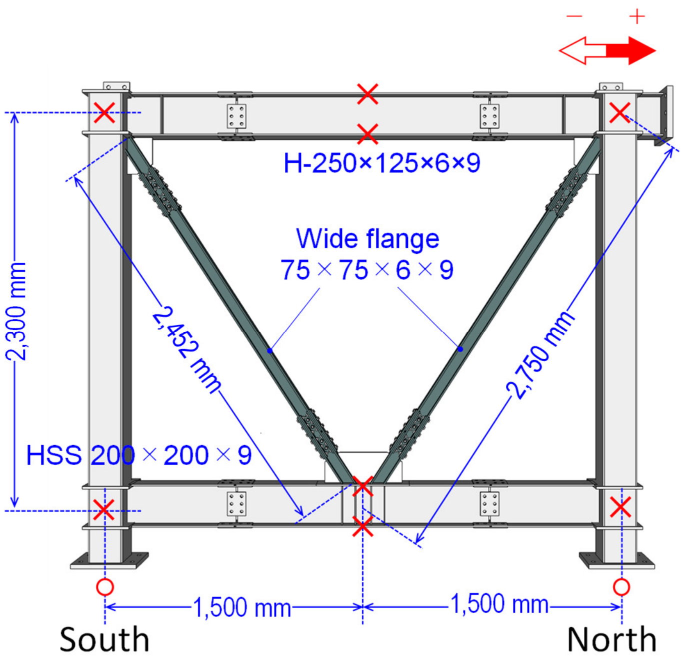

Fig. 4 – Specimen configuration

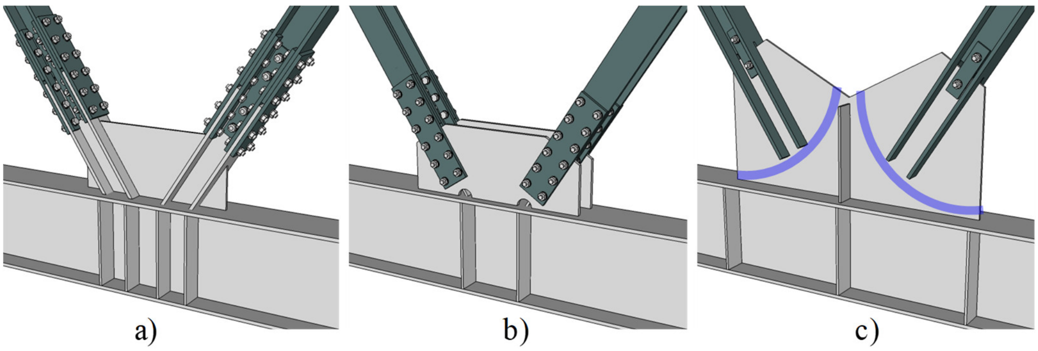

a) b) c)

Fig. 5 – Bracing connections a) Type I; b) Type II; and c) Type III

of ±0.04 rad. The cyclic loading protocol was similar in severity to protocols specified for steel moment-resisting frames in the US provisions [6]. More details about the experiment can be found in [7].

The test results suggest that the structural system combining chevron braces with an MRF can safely develop large cyclic story drifts exceeding 0.03 rad without damage to the bracing connections. The specimens exhibited the weak-beam mechanism, i.e., the braces did not develop their tensile yield strength, and therefore, the bracing connections were not subject to severe tension demands. The beam intersecting the braces yielded and underwent large lateral-torsional deformation and vertical deflection due to the forces transferred by the braces. Therefore, it was suspected that improved performance might be achieved by (a) adopting a stronger beam and thereby achieving a strong-beam mechanism, and (b) enhancing the lateral bracing system of the beam either by reducing the unbraced length or by increasing the stiffness and strength of the bracing system.

4. Parametric Study

A numerical parametric study was conducted to understand the seismic performance of chevron CBFs beyond the parameters examined experimentally. The general-purpose finite element method (FEM) analysis software ADINA [10] was used to carry out the numerical analysis. Fig. 6a outlines the typical three-dimensional FEM model of a test specimen. Details of the modelling and analysis procedure can be found in Dias et al. [11]. The accuracy and reliability of the modelling scheme were validated against the six CBF specimens. Fig. 6b compares the numerical simulation against the experimental response, plotting the relationship between story shear and story-drift angle. The numerical simulation reproduced the experimental behavior quite adequately and, although not illustrated here, captured the global and local deformation observed in the experiment.

A parametric study on the brace-to-beam strength ratio was conducted to establish the limiting ratio κ, in Eqs. (1) and (2), greater than unity, within which yielding of the brace intersecting beam may be controlled. Table 1 lists the 6 chevron-CBF models with varying brace section, bracing connection, and relative horizontal strength of the braces with respect to the beam, r, used for the study. Two different beams, H-250×125×6×9 or H-300×150×6.5×9, with the plastic strength of the latter being 1.4 times that of the former, were combined with 4 different brace sections, either round-HSS or I-section. The brace slenderness ratio λ, taking the node to node distance as the brace length, ranged from 108 to 170 for the round-HSS braces and from 94 to 145 for the I-section braces. Two different bracing connection were used, a bolted detail widely used in Japan (Fig. 5a) and a field welded connection following US recommendations (Fig. 5c).

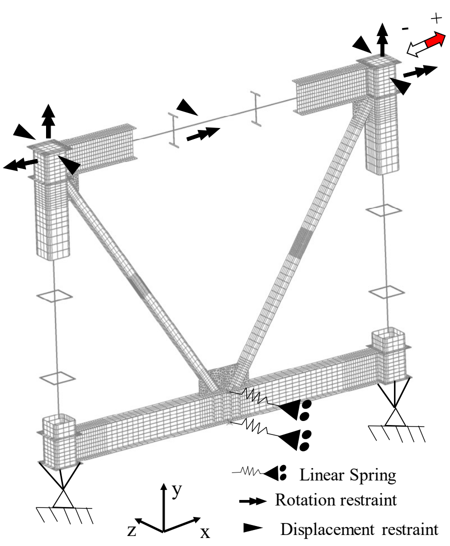

a)

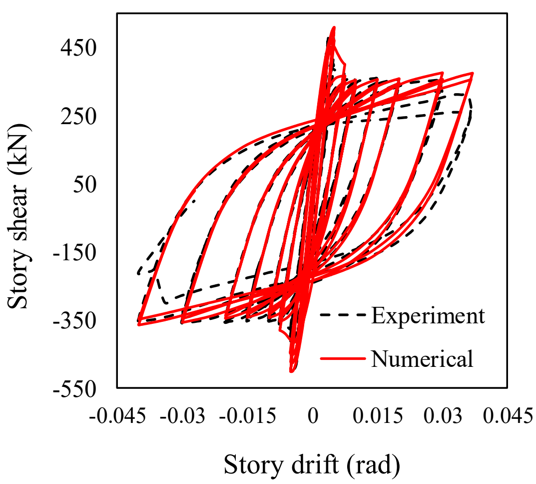

b)

Fig. 6 – FE analysis: a) Typical 3D model of CBF; b) Validation for Specimen 5

Table 1 – Parametric study matrix.

Model	Bracing Connection	Brace	Beam	Column	λ	*r*	Collapse mechanism	β (κ = 1.5)
7	Fig. 5a	H-50×50×4.5×6			142	0.85	Weak beam	0.54
8	Fig. 5c	HSS-76.3×4.2	H-250×150×6×9		108	1.03	Weak beam	0.57
9	Fig. 5a	H-75×75×6×9		Square-HSS-200×200×9	94	1.88	Weak beam	0.69
10	Fig. 5a	H-50×50×2.5×3.2			145	0.34	Strong beam	0.27
11	Fig. 5c	HSS-76.3×2.8	H-300×150×6×9		106	0.50	Strong beam	0.36
12	Fig. 5a	H-75×75×6×9			94	1.34	Weak beam	0.61

The models were numbered starting from 7 for distinction from the specimens numbered 1 to 6. Models 7 and 9 comprised I-section braces with λ =142 and λ = 94, resulting in r = 0.85 and 1.88, respectively, and used the bolted bracing connection. Model 8 comprised tubular braces with λ =108, resulting in r = 1.03, and used the welded bracing connection. Models 10 and 12 comprised I-section braces with λ =145 and λ = 94, resulting in r = 0.34 and 1.34, respectively. Model 11 comprised tubular braces with λ =106, resulting in r = 0.5. Eqs. (1) and (2) for κ = 1.5 imply that the weak-beam mechanism controls for Models 7, 8, 9 and 12, and the strong-beam mechanism controls for Models 10 and 11.

The models were subjected to monotonic pushover and two different cyclic loading protocols: Cyclic-1, which is the same loading protocol used in the experiments was used up to story-drift ratio of 0.04 rad and Cyclic-2, a near field loading protocol which included a smaller number of large excursions but reached 0.04 rad at a much earlier loading stage. The factor β from numerical simulation was computed based on member forces sampled at a fixed loading stage: the end of the first positive excursion at ±0.02 rad for Monotonic and Cyclic-1, and the end of the first positive excursion at ±0.04 rad for the Cyclic-2 loading protocol. The factor κ from numerical simulation was based on the sampled V_b and nominal M_p.

Fig. 7 plots the correlation between β and r from the numerical analysis. The β-r relationship obtained from Eqs. (1) and (2) with κ = 1.5, previously shown in Fig. 3, is shown for comparison. The greatest β and κ from all models was 0.64 and 1.37 in Cyclic-1 analyses, 0.67 and 2.17 in Cyclic-2 analyses, and 0.76 and 2.17 in Monotonic analyses, respectively. Cyclic-2 and Monotonic tended to force the weak-beam mechanism and substantial yielding of the beam. Large overstrength beyond yielding in the beam was the cause of κ exceeding

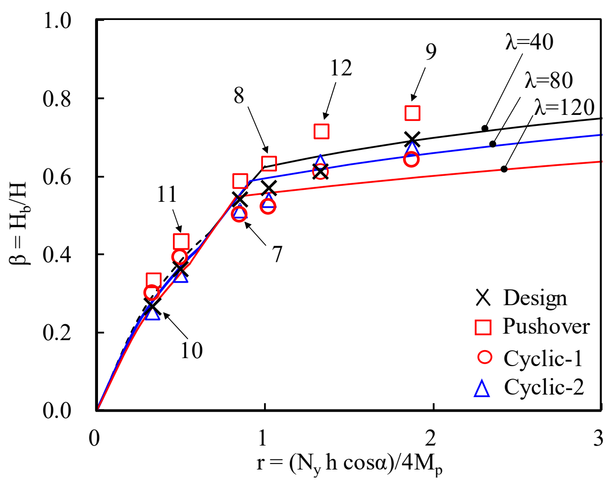

Fig. 7 – Correlation between numerical simulation results and proposed design equation

2 in the analyses. Where the strong-beam mechanism controlled, β was at most 0.43, 0.39 and 0.35 for Monotonic, Cyclic-1 and Cyclic-2, respectively. The observation in Chapter 2 that β should be no greater than 0.4 if yielding of the beam is to be strictly avoided, was validated by the analyses. Where the weak-beam mechanism controlled, κ ranged from 1.3 to 1.37 in Cyclic-1, from 1.56 to 2.17 in Monotonic and from 1.61 to 2.17 in Cyclic-2 while the β-*r* relationship did not deviate far from the design equations with κ = 1.5.

Consequently, the design equations described in Chapter 2 can adequately predict the plastic mechanism and β based on design information *r*. The design equations tended to underestimate β for pushover analysis and overestimate the β for cyclic-loading analysis. Fukuta et al. [12] suggested that κ should be taken as 1.0, stating that design should be on the safe side. If inelastic deflection of the beam intersecting braces is to be strictly avoided, κ should be taken as 1.0, as suggested by Fukuta et al. [12], and β cannot exceed 0.4. However, the numerical results suggest that κ = 1.5, which permits more economic design, may secure adequate performance.

5. System Performance of Low-rise Chevron Braced Frame

The system level performance of chevron CBFs was examined by nonlinear time history analyses of the 4-story office building depicted in Fig. 8. The lateral-load resisting system comprised two exterior MRF bays and one inner chevron CBF bay. In the following discussion, β is evaluated for the braced bay only and do not account for the contribution of the exterior bays, which was within 15% of the total lateral-load resistance.

The CBFs were proportioned according to the assumed mechanisms illustrated in Fig. 9: Case A where the brace tension and compression both equals N_{cr}; Case B where the beam is proportioned not to yield due to the force imbalance under brace tension N_y and brace compression $N_u = 0.3N_{cr}$; Case C where partial yielding of the beam is allowed under brace tension N_t (< N_y) and brace compression N_u; and Case D where the beam is simply supported and proportioned to remain elastic under brace tension N_y and brace compression N_u. Case A, which assumes no force unbalance between the braces, does not reflect the true mechanism. Nonetheless,

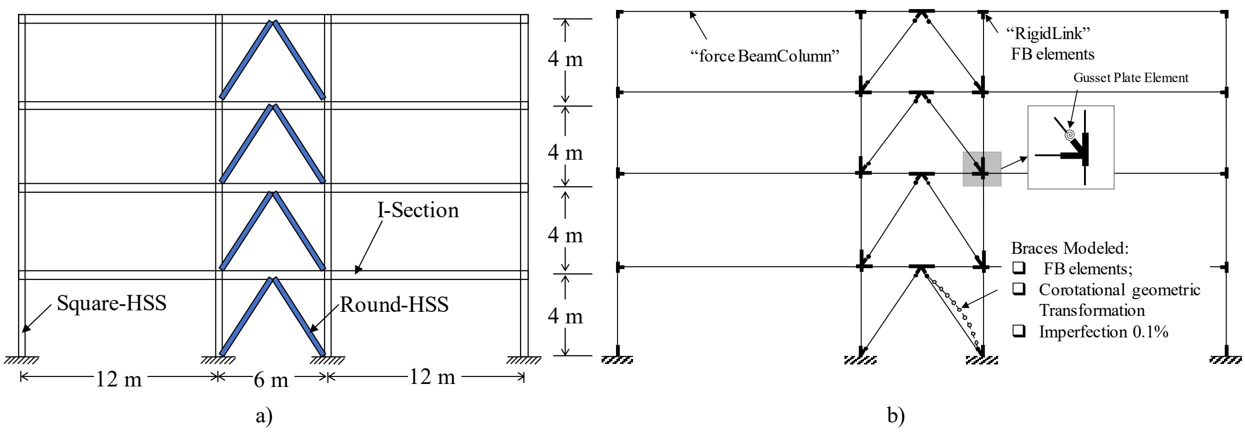

Fig. 8 – Four story frame: a) Building configuration; b) Analytical model

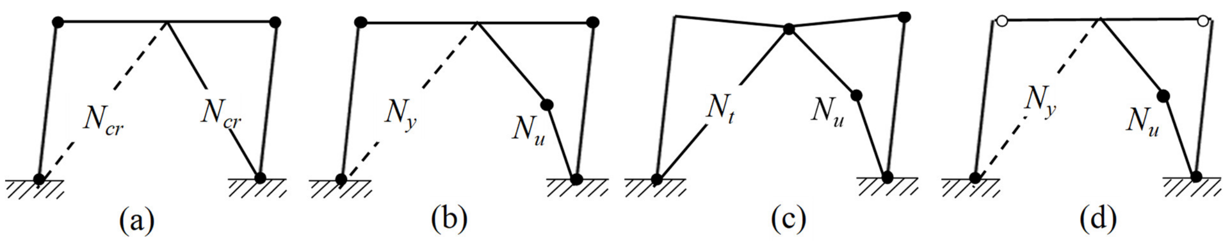

Fig. 9 – Design approach for the braced frame design: (a) Case A; (b) Case B; (C) Case C; and (d) Case D

Case A was permitted in Japan until 2015 and adopted by many engineers until that time. Case B to D addresses the need to proportion the beam for the force unbalance. Case B requires the beam to remain elastic, and is possible only for $\beta < 0.4$ per the earlier discussion. Case C permits yielding of the beam up to $\kappa = 1.5$ and is possible only for $0.4 < \beta < 0.7$ per the earlier discussion. Case D is the option adopted in North America which, in theory, achieves $\beta = 0.7$. In general, for the same β, the cross-sectional area of braces is larger in the order of Case D, C, B, then A. Case D requires larger braces because the braces are the only source of lateral-load resistance. Only in Case D, the proportioning rule for the beams is a statically determinant problem.

Three different values were adopted for β, 0.35, 0.65 and 1.0. Case A adopted either $\beta = 0.35$ or 0.65, Case B adopted $\beta = 0.35$, Case C adopted $\beta = 0.65$ and Case D naturally adopted $\beta = 1.0$. Cases A and B with $\beta = 0.35$ resulted in nearly identical design.

The gravity loads comprised uniformly distributed dead load of 8 kN/m^2 and live load of 2.4 kN/m^2. The design earthquake loads were determined according to the Level-2 design of the Japanese Building Standard [13]. The structural characteristic coefficient, D_s, was set as 0.3 assuming that the member ductility class of the braces were BB and the moment-resisting frames were FB. The braces were tubular hollow structural sections (HSS) with a fixed diameter-to-thickness ratio of $d/t = 33$. The brace slenderness ratio KL/r ranged from 68 to 100, 48 to 81, and 41 to 61, for $\beta = 0.35$, 0.65, and $\beta = 1.0$, respectively.

Analysis was conducted using OpenSees [14]. Force-based beam-column elements were adopted for all the columns, beams and braces. The beams and columns were modelled with a single element with five integration points arranged according to the Gauss-Lobatto quadrature rule. Each flange or web element was divided into eight elements, four in the width direction and two in the thickness direction. The braces were modelled by two elements whose cross section was discretised into 12 elements in the circumferential direction and 4 elements in the radial direction, with an initial imperfection of 0.1% of the brace length. Corotational transformation was used in the braces and the beams elements, while P–delta transformation was used in the columns. The uniaxial stress-strain relationship assigned to each fiber adopted the Menegotto-Pinto rule with the parameters calibrated based on cyclic-loading material tests by Yamada et al. [15]. Fig. 10 illustrates the modelling scheme for each bracing connection. The segments stiffened by gusset plate was modelled as rigid. Type II had the brace rigidly connected at the ends; Types I and III were modelled with a zero-length spring as done by Hsiao et al. [16]. The loading protocol and boundary conditions were same as the experiment.

The modelling scheme was validated using the experimental data and FEM simulation of the single story-single bay frames discussed previously. Fig. 11 compares the OpenSees, FEM and experimental response for Specimens 2 and 3, which adopted bracing connection Types II and III, respectively. The figure shows that, the two-dimensional OpenSees simulation slightly overestimated the buckling strength of braces and underestimated their post-buckling strength but otherwise showed good agreement with the experimental and FEM simulation. The figure indicates that bracing connection Type II, which unlike Type III provides large fixity at the brace ends, leads to larger compressive strength and post buckling strength of the braces. Although

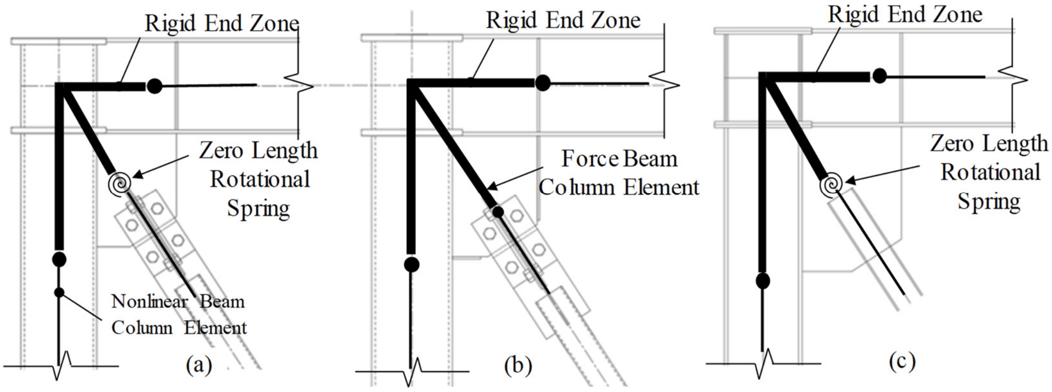

Fig. 10 – Modelling scheme of the bracing connections: a) Type I; b) Type II; c) Type III

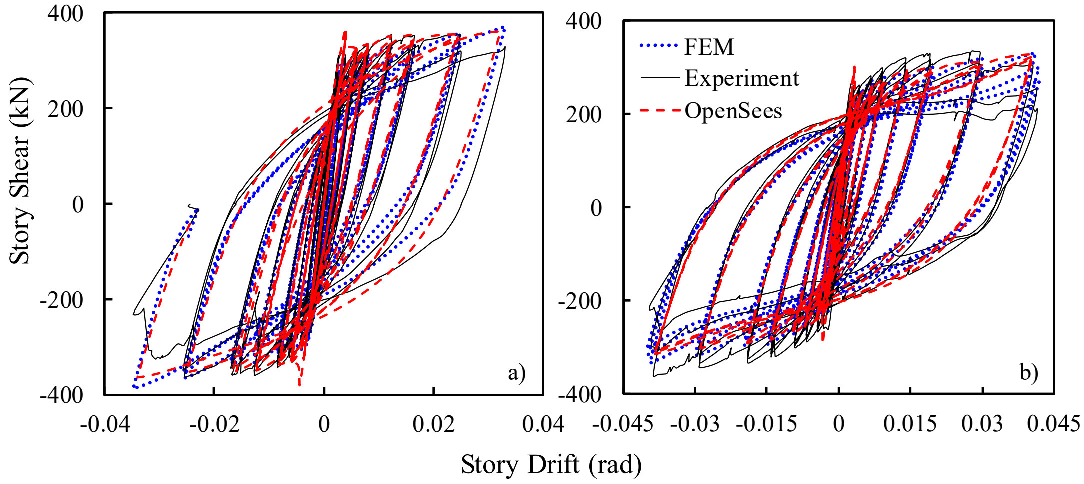

Fig. 11 – Model validation: a) Specimen 2; b) Specimen 3

not shown in the figure, the difference between bracing connections Types I and III was small: Type III with larger gusset plate leads to somewhat shorter beams, columns and braces but the difference hardly affected the analysis results.

Fig. 12 shows the base shear versus story drift response obtained from nonlinear pushover analysis with load distribution according to the A_i rule of the Japanese Building Standard [13]. The figure compares four CBF models that adopted different design assumptions and β values, but all employed bracing connection Type I. The reference line indicates the design base shear. All models exceeded the design base shear, which was based on a base shear coefficient of 0.3. As stated earlier, Case A with β = 0.35 was nearly identical to Case B with β = 0.35 and is therefore omitted in this comparison. For Case B with β = 0.35, the simulated β at 0.02-rad roof drift was 0.28, 0.29, 0.32, 0.33 for stories 1 to 4, respectively. The simulated κ was no greater than 0.77, and accordingly, the braces in all stories yielded in tension and none of the beams yielded. For Case C with β = 0.65, the simulated β at 0.02-rad roof drift equalled 0.48, 0.52, 0.57, 0.45 for stories 1 to 4, respectively. The simulated κ was no greater than 1.7. The braces in the first to third stories yielded in tension but developed limited extension. None of the beams yielded but developed significant elastic vertical deflection. For the same β = 0.65, Case C resulted in a 30% stronger system than Case A, and more uniform distribution of story drift across the height. For Case D with β = 1.0, although the model was substantially

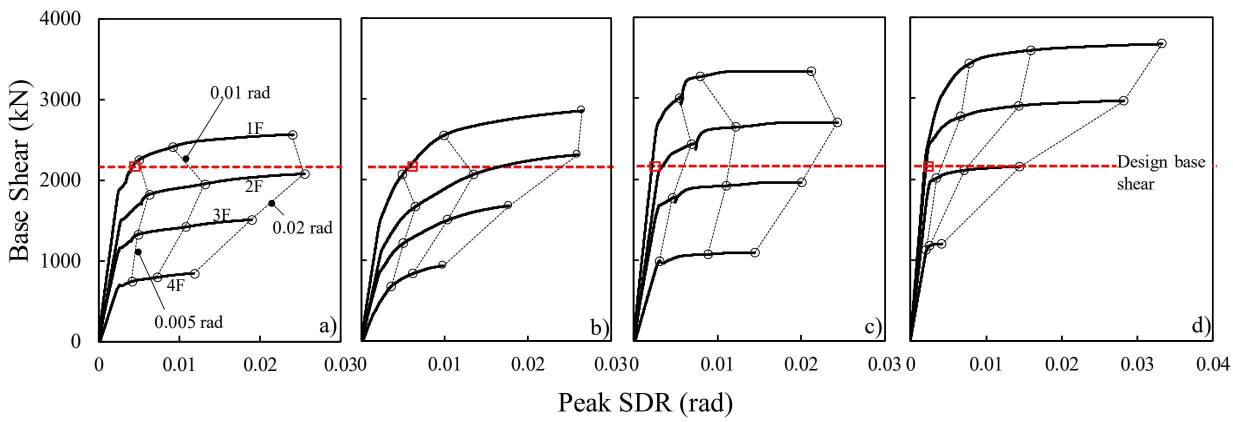

Fig. 12 – Pushover curves of CBFs with bracing connection type I: a) Case A with β = 0.65; b) Case B with β = 0.35; c) Case C with β = 0.65; d) Case D

stronger than the other cases depicted in the figure, the braces yielded in tension only in the first and second stories.

The effect of bracing connection type was more significant in the order of Case D, C, B and A. The difference between Cases A and B was small. For Case C, the use of bracing connection Type II over Type I led to 6% larger story shear for $\beta = 0.35$ and 22% larger for $\beta = 0.65$.

Nonlinear time history analysis was performed on the models using the four ground motions listed in Table 2, of which three are records from past earthquakes and one is artificial. The artificial BCJ-L2 is very commonly used in the engineering practice in Japan. The constant average acceleration scheme was used for integration over time. Rayleigh damping with a critical damping ratio of $\zeta = 0.02$ was assigned to the first two modes. The seismic mass was computed as 100% of dead load and 25% of live load.

Fig. 13 plots the distribution of maximum story drift rotation obtained for Cases A, B and C, all with $\beta = 0.65$ and employing bracing connection Type I. The models deformed beyond story drift ratio of 0.02 rad under the Kumamoto record, but remained within 0.02 rad for the other three records. Notable difference was observed for the Kumamoto earthquake record where Case C developed much larger story drifts than Cases A and B. Contrary to Kumamoto, JMA Kobe record caused Case B to develop the largest deformation and Case C the smallest. For the Kumamoto record, Case C developed brace yielding in the second and third stories and the beams at second to fourth floors yield due to force unbalance.

Table 2 – Ground motions

Name	Component	Year, Recording Site	PGA (m/s^2)	Duration (s)
JMA Kobe	NS	1995, Southern Hyogo Prefecture	0.82	8.3
Kumamoto	EW	2016, KiK-NET Mashiki	1.16	60
BCJ-L2	-	--	0.36	65.4
Northridge	NS	1994, USGS 0793	0.38	10

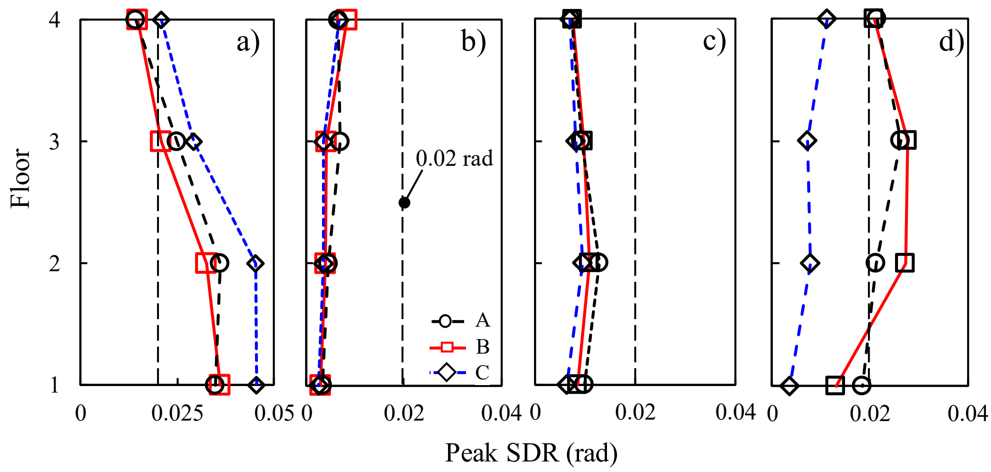

Fig. 13 – Maximum SDR for models with $\beta = 0.65$ and bracing connection Type I from records: a) Kumamoto; b) Northridge; c) BCJ-L2 and d) JMA Kobe

6. Conclusions

The seismic performance of typical Japanese CBFs was examined by FEM simulation of a substructure and time history analysis of a four-story building system. The effect of key design parameters such as the relative horizontal strength of the braces with respect to the beam, r, the proportion of lateral strength derived from the braces when a full mechanism is formed, β, $0 \leq \beta \leq 1$, and the strength of the beam intersecting braces with respect to the braces, κ, $1 \leq \kappa \leq 2$, was evaluated. Among the three parameters, β and κ depend on the loading history. The main findings of the analyses can be summarized as follows:

- A design equation was proposed to relate r with β. The equation can reliably predict the plastic mechanism and β by assuming $\kappa = 1.5$. If inelastic deformation of the beam is to be avoided, β should be no greater than 0.4 and κ should be taken as unity. However, $\kappa = 1.5$ may permit more economic design.
- For $\beta = 0.35$, the design based on a simplistic mechanism where both the tension and compression braces develop the buckling strength may not lead to problematic behavior. At such low β, regardless of whether force unbalance is considered or not, the strong-beam mechanism tended to control.
- For $\beta = 0.65$, which calls for large brace sections, the force imbalance was so large that weak-beam mechanism tended to control. Such design may not be realized unless κ is set greater than unity. A reasonable value is $\kappa = 1.5$.
- For $\beta = 1.0$, which is realized only when the beam is simply connected to the column, elongation of the braces was limited by elastic deflection of the beam.
- For all combination of design cases and β, the story drift produced by ground motions with elastic acceleration response spectrum of up to 1.2g at the fundamental vibration frequency was within 0.02 rad. Therefore, all models met the design requirements stipulated by the Japanese code.

Work is ongoing to expand the numerical simulation by including brace and beam fracture.

7. References

[1] Shibata M, Wakabayashi M (1983): Experimental study on the hysteretic behavior of k-type braced frame subjected to repeat load. *Transactions, Architectural Institute of Japan*, **326**, 10-16 (in Japanese).

[2] Yamanouchi H, Midorikawa M, Nishiyama I, Watabe M (1989): Seismic behavior of full-scale concentrically braced steel building structure. *Journal of Structural Engineering*, ASCE, **115** (8), 1917-1929.

[3] Fukuta T, Nishiyama I, Yamanouchi H (1989): Seismic performance of steel frames with inverted V braces, *Journal of Structural Engineering*, ASCE, **115** (8), 2016-2028.

[4] Khatib IF, Mahin S, Pister KS (1988): Seismic behavior of concentrically braced steel frames, PEER Report 1988/01, Berkeley, CA, USA.

[5] Tremblay R, Roberts N (2001): Seismic performance of low and medium-rise chevron braced steel frames, *Canadian Journal of Civil Engineering*, **28**: 699-714.

[6] American Institute of Steel Construction, Inc (AISC). (2016): Seismic provisions for structural steel buildings. ANSI/AISC *Standard 341-16*, Chicago, Illinois.

[7] Seki A, Okazaki T, Dias I, Hayato A (2018): Experimental behavior of chevron braced frames designed according to current practice. *Japan Association of Earthquake Engineering*.

[8] Architectural Institute of Japan (AIJ) (2010): *Recommendations for Limit State Design of Steel Structures*, AIJ, Tokyo, Japan (in Japanese).

[9] Roeder CW, Lumpkin EJ, Lehman DE (2011): A balanced design procedure for special concentrically braced frame connections. *Journal of Constructional Steel Research*, **67**, 1760-1772.

[10] ADINA R&D, Inc. (2017): *Theory and Modelling Guide*. ADINA 9.3.

[11] Dias I, Akiri S, Okazaki T (2019): A Computational study on the cyclic loading behavior of steel chevron braced frames. *12th Pacific Structural Steel Conference*, Tokyo, Japan.

[12] Fukuta T, and Yamanouchi H (1989): Ultimate lateral shear capacity of steel frames with inverted V-braces, *Journal of Structural and Construction Engineering*, (398), 99-106.

[13] Building Center of Japan (BCJ) (1997): *Structural Provisions for Building Structures*, Tokyo, Japan.

[14] McKenna F (1997): Object oriented finite element programming frameworks for analysis, algorithms and parallel computing. *Ph.D. Dissertation*, Univ. of California, Berkley, USA.

[15] Yamada S, Imaeda T, Okada K (2002): Simple hysteresis model of structural steel considering the Bauschinger effect. *Journal of Structural and Construction Engineering*, 559, 225-232 (in Japanese).

[16] Hsiao P C, Lehman D E, and Roeder C W (2012): Improved analytical model for concentrically braced frames. *Journal of Constructional Steel Research*, **73**, 80-94.

